NEURO

Arterial transit artifacts on arterial spin labeling MRI can predict cerebral hyperperfusion after carotid endarterectomy: an initial study

Xiaoyuan Fan[1] · Zhentao Zuo[2,3] · Tianye Lin[1] · Zhichao Lai[4] · Hui You[1] · Jianxun Qu[5] · Juan Wei[5] · Bao Liu[4] · Feng Feng[1,6]

Abstract

Objectives To investigate whether preoperative arterial spin labeling (ASL) MRI can predict cerebral hyperperfusion after carotid endarterectomy (CEA) in patients with carotid stenosis.

Methods Consecutive patients with carotid stenosis who underwent CEA between May 2015 and July 2021 were included. For each patient, a cerebral blood flow ratio (rCBF) map was obtained by dividing postoperative CBF with preoperative CBF images from two pseudo-continuous ASL scans. Hyperperfusion regions with rCBF > 2 were extracted and weighted with rCBF to calculate the hyperperfusion index. According to the distribution of the hyperperfusion index, patients were divided into hyperperfusion and non-hyperperfusion groups. Preoperative ASL images were scored based on the presence of arterial transit artifacts (ATAs) in 10 regions of interest corresponding to the Alberta Stroke Programme Early Computed Tomography Score methodology. The degree of stenosis and primary and secondary collaterals were evaluated to correlate with the ASL score. Logistic regression and receiver operating characteristic curve analyses were performed to assess the predictive ability of the ASL score for cerebral hyperperfusion.

Results Of 86 patients included, cerebral hyperperfusion was present in 17 (19.8%) patients. Carotid near occlusion, opening of posterior communicating arteries with incomplete anterior semicircle, and leptomeningeal collaterals were associated with lower ASL scores ($p < 0.05$). The preoperative ASL score was an independent predictor of cerebral hyperperfusion (OR = 0.48 [95% CI [0.33–0.71]], $p < 0.001$) with the optimal cutoff value of 25 points (AUC = 0.98, 94.1% sensitivity, 88.4% specificity).

Conclusions Based on the presence of ATAs, ASL can non-invasively predict cerebral hyperperfusion after CEA in patients with carotid stenosis.

Key Points

• *Carotid near occlusion, opening of posterior communicating arteries with incomplete anterior semicircle, and leptomeningeal collaterals were associated with lower ASL scores.*

• *The ASL score performed better than the degree of stenosis, type of CoW, and leptomeningeal collaterals, as well as the combination of the three factors for the prediction of cerebral hyperperfusion.*

• *For patients with carotid stenosis, preoperative ASL can non-invasively identify patients at high risk of cerebral hyperperfusion after carotid endarterectomy without complex post-processing steps.*

✉ Zhichao Lai
zhichao_lai@126.com

✉ Feng Feng
cjr.fengfeng@vip.163.com

[1] Department of Radiology, Peking Union Medical College Hospital, Chinese Academy of Medical Sciences and Peking Union Medical College, No. 1 Shuaifuyuan, Wangfujing, Dongcheng District, Beijing 100730, China

[2] State Key Laboratory of Brain and Cognitive Science, Institute of Biophysics, Chinese Academy of Sciences, Beijing, China

[3] Sino-Danish College, University of Chinese Academy of Sciences, Chinese Academy of Sciences, Beijing, China

[4] Department of Vascular Surgery, Peking Union Medical College Hospital, Chinese Academy of Medical Sciences and Peking Union Medical College, No. 1 Shuaifuyuan, Wangfujing, Dongcheng District, Beijing 100730, China

[5] GE Healthcare, MR Research China, Beijing, China

[6] State Key Laboratory of Difficult, Severe and Rare Diseases, Peking Union Medical College Hospital, Chinese Academy of Medical Sciences and Peking Union Medical College, Beijing, China

🖄 Springer

Abbreviations

ASL	Arterial spin labeling
ATA	Arterial transit artifact
BP	Blood pressure
CBF	Cerebral blood flow
CEA	Carotid endarterectomy
CHS	Cerebral hyperperfusion syndrome
CoW	Circle of Willis
CVR	Cerebrovascular reactivity
FHV	Fluid-attenuated inversion recovery hyperintense vessel
FLAIR	Fluid-attenuated inversion recovery
HI	Hyperperfusion index
PLD	Post-labeling delay

Introduction

As a rare but serious complication after carotid revascularization, cerebral hyperperfusion syndrome (CHS) is an important cause of postoperative hemorrhagic stroke. CHS often occurs in patients with cerebral hyperperfusion, defined as an increase of more than 100% in perfusion compared with baseline [1, 2]. The most accepted mechanism of cerebral hyperperfusion is impaired cerebrovascular reactivity (CVR) [2], which cannot maintain a stable cerebral blood flow (CBF) via vasoconstriction in response to a sudden increase of cerebral perfusion pressure after revascularization. Preoperative measurement of CVR using acetazolamide or CO_2-induced single-photon emission computerized tomography (SPECT) is the gold standard for predicting cerebral hyperperfusion after carotid endarterectomy (CEA) [1, 3, 4]. However, it is often impractical to perform CVR examinations on all patients, considering the potential side effects of acetazolamide or CO_2 [5, 6].

In recent years, various of techniques have been applied to replace the use of SPECT for predicting cerebral hyperperfusion after carotid revascularization, including transcranial Doppler [7], color-coded digital subtraction angiography (DSA) [8], blood sampling from the carotid artery [9], and near-infrared spectroscopy [10]. However, these methods have not been implemented in clinical practice for CEA patients due to technical limitations. The inadequacy of transtemporal bone windows often limits the use of transcranial Doppler. DSA and blood sampling are invasive, and near-infrared spectroscopy needs the injection of indocyanine green kinetics.

Arterial spin labeling (ASL) is a non-invasive technique to image the brain perfusion by using magnetically labeled arterial blood as endogenous tracer. ASL can provide CBF values comparable to SPECT in various types of cerebrovascular disease [11, 12]. The flaw of ASL is the sensitivity to arterial arrival time. If arterial arrival time is longer than the post-

labeling delay, labeled blood will remain in vessels at the time of imaging. It appears as bright serpiginous or spotted intravascular signals on ASL images, the so-called arterial transit artifacts (ATAs) (Fig. 1) [13]. However, this "artifact" actually can be a helpful imaging marker as it often indicates delayed arrival of blood in the corresponding vascular territory caused by stenosis or collateral pathways [14].

Based on the presence of ATAs, Zaharchuk et al developed a reliable ASL score for the evaluation of collateral flow [13, 15]. In the case of severe carotid stenosis and deficient collateral flow, cerebral perfusion pressure is severely decreased distal to the stenosis, even below the compensatory capacity of autoregulatory mechanisms. That often causes misery perfusion and exhausted CVR [16–18]. Preoperative poor collateral conditions increase the risk of hyperperfusion after carotid revascularization [19, 20].

The purpose of the study was to determine whether this ATA–based ASL score can predict cerebral hyperperfusion after CEA in patients with carotid stenosis. We hypothesized that the ATA–based ASL score contained important information of collateral flow and preoperative ASL images may be a potential non-invasive approach to predict cerebral hyperperfusion after CEA.

Materials and methods

This prospective study was approved by the Medical Ethics Committee of the Peking Union Medical College Hospital, in line with the Declaration of Helsinki. All subjects provided written informed consent for this study.

Patients

From May 2015 to July 2021, consecutive patients undergoing CEA for carotid stenosis ($\geq$ 50% for symptomatic stenosis or $\geq$ 70% for asymptomatic stenosis, according to the North American Symptomatic Carotid Endarterectomy Trial [NASCET] grading) diagnosed with computed tomography angiography (CTA) were included. Patients underwent MRI within 2 weeks before CEA and within 7 days after CEA. The exclusion criteria were as follows: (1) patients with MRI contraindications or who did not finish two MRI scans in the proper time; (2) intracranial artery stenosis ($\geq$ 50%) or occlusion shown by preoperative CTA; (3) ipsilateral ischemic lesions that occupy $\geq$ 1 complete cortical region based on the Alberta Stroke Programme Early Computed Tomography Score (ASPECTS) on preoperative MRI; (4) postoperative prevention or treatment of CHS including intravenous antihypertensive drugs, mannitol, or glycerol fructose for a long period ($\geq$ 5 days) before the MR scan; and (5) artifacts on MRI.

Fig. 1 Representative images of arterial spin labeling (ASL) with arterial transit artifacts (ATAs) and normal ASL without ATAs
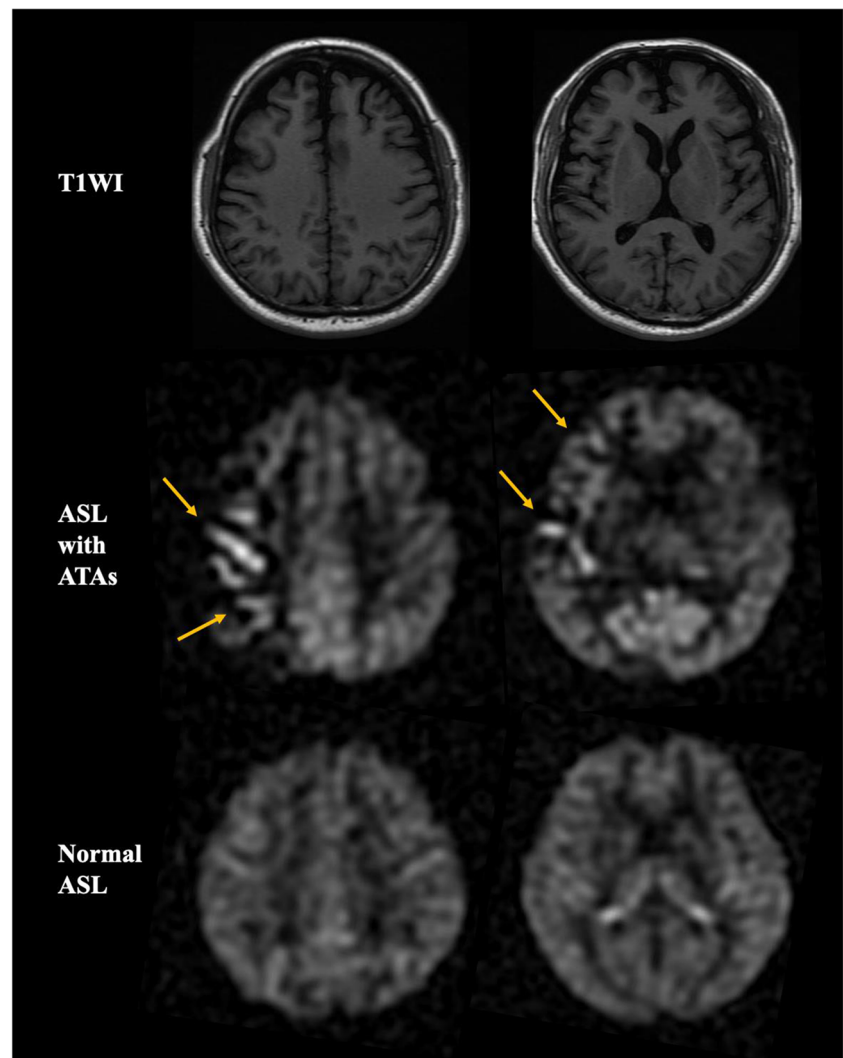
MRI

All MRI examinations were performed on a 3.0-T scanner (Discovery 750, GE Healthcare) equipped with an eight-channel phase-array head coil. Background suppressed pseudo-continuous ASL (a 3D stack-of-spirals fast-spin-echo readout, without vascular crushing, labeling duration/post labeling delay [PLD] = 1450/2025 ms, TR/TE = 4886/10.5 ms, in-plane spiral arms number 8, 512 points per spiral arm, field of view = 240 × 240 mm^2, nominal in-plane resolution 3.75 × 3.75 mm^2, 40 slices and slice thickness = 4 mm) was performed. ASL CBF maps were generated from the 3D ASL Functool software (AW 4.5 Workstation, GE Healthcare). The 3D T1-weighted MRI was acquired by inversion-prepared fast spoiled gradient echo with isotropic resolution of 1 mm, 170 slices, TI/TR/TE = 400/6.6/2.9 ms, flip angle = 12°, field of view = 256 × 230 mm^2. Routine 3D time-of-flight MR angiography, diffusion-weighted imaging, T1-weighted, T2-weighted, and fluid-attenuated inversion recovery (FLAIR) were also performed (Table S1).

ASL score and relevant imaging features

The preoperative ASL images were graded on 2 slices corresponding with the ASPECTS locations using a 4-point scoring system as follows: 0, no or minimal ASL signal; 1, low/moderate ASL signal with ATA; 2, high ASL signal with ATA; and 3, normal perfusion without ATA [13]. Several slices immediately above and below the precise ASPECTS slice were checked to improve the robustness of this scoring system [13]. This grading was performed in 10 cortical regions in the ipsilateral hemisphere of surgery, and the overall ASL score ranged from 0 to 30 (two cases in Figs. 5 and 6 are for reference). Two radiologists with 19 and 7 years of experience in neuroradiology independently evaluated the ASL score, blinded for the clinical and other imaging information. Disagreements were resolved by consensus. To assess intra-observer variability, one observer reviewed the same ASL images of 69 patients included from May 2015 to January 2021 (3 months apart).

The degree of stenosis was measured on CTA. Moderate and severe stenoses were determined according to the NASCET criteria [21]. An interpretive approach was used to identify the presence of carotid near-occlusion based on previous studies [22, 23]. Carotid near-occlusion was diagnosed conservatively by two radiologists only when the diagnosis was the most reasonable.

The presence of collateral flow routes in the circle of Willis (CoW) was assessed with MR angiography. The anterior communicating artery (ACom), both sides of the first segment of the anterior cerebral arteries (A1), the first segment of the ipsilateral posterior cerebral artery (P1), and the ipsilateral posterior communicating artery (PCom) were evaluated [24]. The anterior semicircle of the CoW was complete if the ACom and both sides of the A1 were definitely present. The posterior semicircle was complete if the ipsilateral P1 and PCom were definitely present. The CoW was divided into four types: type 1, complete anterior semicircle and complete posterior semicircle; type 2, complete anterior semicircle and incomplete posterior semicircle; type 3, incomplete anterior semicircle and complete posterior semicircle; and type 4, incomplete anterior semicircle and incomplete posterior semicircle. The secondary leptomeningeal collaterals were determined based on the presence of ipsilateral fluid-attenuated inversion recovery hyperintense vessels (FHVs) [25]. FHV was defined as a linear high-signal intensity along the cortical sulci or brain surface in the cerebral hemisphere on FLAIR images (the case in Fig. 5 is for reference) [26]. FHVs extended to the frontal-parietal lobes were conservatively diagnosed as opening of leptomeningeal collaterals [27]. The type of CoW and opening of leptomeningeal collaterals were assessed by an experienced radiologist, blinded for the ASL score and clinical information.

Diagnosis of cerebral hyperperfusion and CHS

For the diagnosis of cerebral hyperperfusion, images were analyzed using MATLAB (MathWorks) and SPM12 (Wellcome Department of Cognitive Neurology, Institute of Neurology). Firstly, the non-labeled ASL images were registered to the 3D T1-weighted space and then the transformation matrix was performed on preoperative and postoperative CBF images. A CBF ratio map was generated through dividing the postoperative CBF map with the preoperative CBF map on the voxel level in the whole brain. To avoid the impact of ATAs for overestimating CBF, voxels with CBF > 70 ml/ (100 g·min) on the preoperative CBF map were excluded [28]. Then, the CBF ratio maps and 3D T1-weighted images were normalized to the Montreal Neurological Institute space and masked with an arterial flow territory template to extract hyperperfusion regions from gray matter in the entire ipsilateral middle cerebral artery territory [29]. To eliminate the influence of image noise, only clusters larger than 100 mm³

with all voxels CBF ratio > 2 were extracted as effective hyperperfusion region [2]. Then the hyperperfusion index (HI) for each patient was acquired by summing the products of the CBF ratio and volume for each voxel in hyperperfusion regions.

According to the distribution of HI among included patients (Fig. 2b), the last 17 patients with significantly higher HIs (log HI > 4.5) were grouped as cerebral hyperperfusion. The overview of processing steps with two representative cases is shown in Fig. 2.

CHS was defined as follows: (1) existence of cerebral hyperperfusion; (2) clinical features such as ipsilateral throbbing headache, seizures, deterioration of consciousness level, focal neurological signs, or intracranial hemorrhage; and (3) no evidence of new ischemic lesions on postoperative MRI.

Statistical analysis

All data was analyzed using statistical software (IBM SPSS v25.0 and MedCalc v20.09). Patient characteristics were expressed as means ± standard deviation, numbers of patients and percentages, or medians and interquartile range. Linear-weighted κ values were calculated for the inter-observer and intra-observer agreements of the ASL score.

The Mann-Whitney U test and Kruskal-Wallis H test were used to evaluate the relationship between the degree of stenosis, different types of CoW, leptomeningeal collaterals, and ASL score, as appropriate. Bonferroni correction was performed for multiple comparisons. Univariable binary analysis was used to examine potential risk factors for cerebral hyperperfusion. To determine the association of the ASL score with hyperperfusion adjusted for other risk factors, age, sex, and variables with $p <$ 0.2 in univariate analysis were entered into a forward stepwise logistic regression model. The primary interest was in the relationship between the ASL score and cerebral hyperperfusion. Therefore, as the ASL score was considered to be a comprehensive imaging marker related to stenosis and the primary and secondary collaterals, we did not include the degree of stenosis, type of CoW, and leptomeningeal collaterals into the multivariate logistic regression model. Spearman correlation analysis was used to evaluate the relationship between the ASL score and Log HI.

Receiver-operating characteristic (ROC) analysis was used to assess the predictive ability of the degree of stenosis, type of CoW, leptomeningeal collaterals, combination of the three factors, and ASL score. The areas under the curve (AUCs) of predictors were compared by using the Delong test. The optimal cutoff value of the ASL score for predicting cerebral hyperperfusion was determined by maximizing the Youden index. For patients with hyperperfusion, Student's t test, Mann-Whitney U test, and Fisher exact test were used for univariable analysis between the CHS group and non-CHS
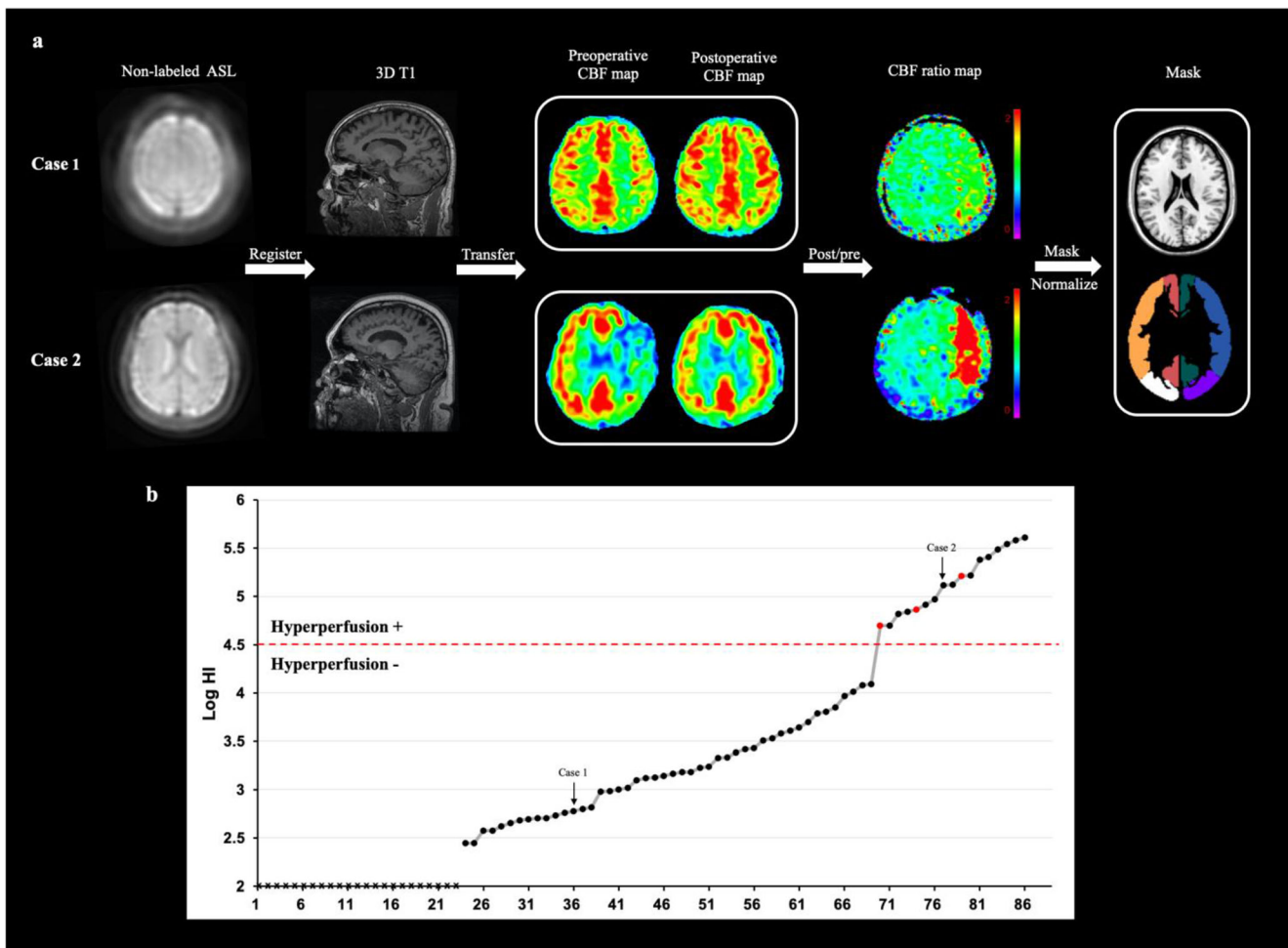
Fig. 2 Overview of processing steps with two representative cases. **a** Preoperative and postoperative cerebral blood flow (CBF) maps were registered to non-labeled arterial spin labeling (ASL) and 3D T1 space and then divided to generate CBF ratio maps. CBF ratio maps were normalized and masked with a cerebral flow territory template to acquire hyperperfusion volume in the ipsilateral middle cerebral artery territory. **b** The distribution of hyperperfusion indexes (HI) among 86 included patients. Case 1 was identified as non-hyperperfusion, case 2 was identified as hyperperfusion. Red dots indicate patients with cerebral hyperperfusion syndrome. A cross indicates HI is 0

group. All p values were calculated using two-tailed tests. A value of $p < 0.05$ was considered statistically significant.

Results

Participant characteristics and inter- and intra-observer agreements

From May 2015 to July 2021, 111 patients were initially included in the study. Among the 111 patients, 7 had MRI contraindications, 5 did not finish two MRI scans, 5 were observed with intracranial artery stenosis or occlusion on preoperative CTA, 2 had massive ischemic stroke, 1 had postoperative treatment with mannitol for 7 days before MRI, and 5 had artifacts on the ASL images. A final 86 patients were enrolled for analysis (Fig. 3). The mean age of the included patients was 65.3 ± 7.1 years, and 75.6% were male. Thirty-two patients (37.2%) had symptomatic carotid stenosis. CEA was successfully performed in all patients. Cerebral hyperperfusion was present in 17 (19.8%) patients. Hyperperfusion occurred most frequently in the distal flow territory of the middle cerebral artery (M4–6) and watershed area (Figure S1). The characteristics of the study population are shown in Table 1.

Inter-observer ($\kappa = 0.72$, 95% CI [0.68–0.77]) and intra-observer ($\kappa = 0.83$, 95% CI [0.80–0.87]) agreements for the ASL score were good and excellent.

ASL score, degree of stenosis, primary and secondary collaterals

The association between the ASL score and the degree of stenosis and primary and secondary collaterals is shown in Table 2. Patients with carotid near occlusion had lower ASL scores than those with moderate (adjusted $p = 0.01$) or severe

Fig. 3 Flowchart of patient enrollment
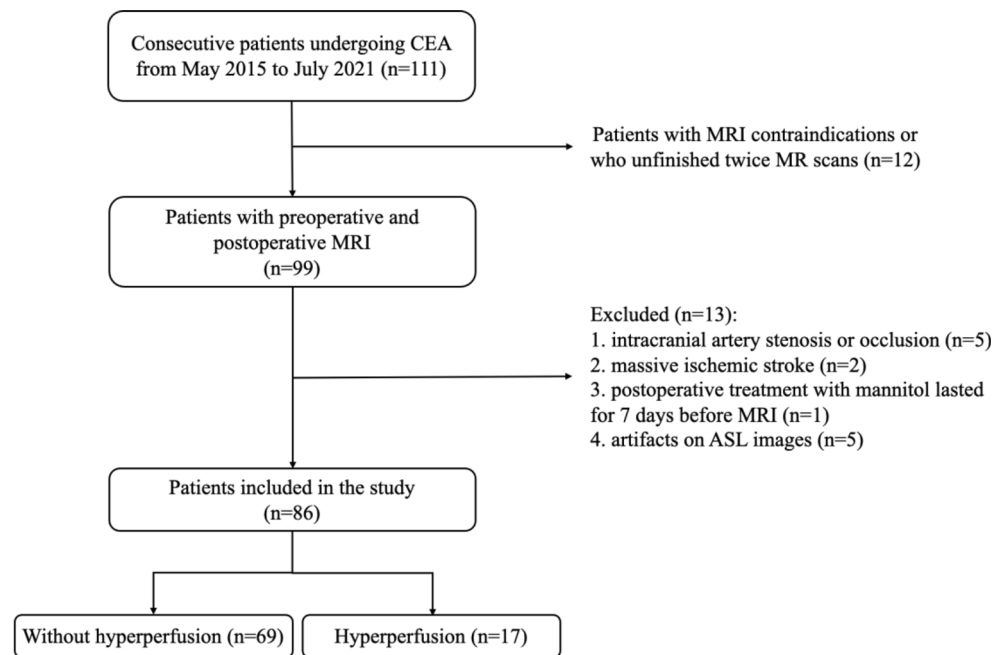
stenosis (adjusted $p = 0.003$). Patients with an incomplete anterior semicircle (type 3 and type 4, median ASL score = 26 [19.5, 29]) had lower ASL scores than those with a complete anterior semicircle (type 1 and type 2, median ASL score = 28 [27, 30], $p = 0.006$). In particular, the ASL scores were significantly lower in patients with type 3 CoW than in the other three types (type 1, adjusted $p = 0.001$; type 2, $p = 0.003$; type 4, $p = 0.028$). Patients with leptomeningeal collaterals had significantly lower ASL scores than those without leptomeningeal collaterals ($p < 0.001$).

Association between ASL score and cerebral hyperperfusion

Patients with hyperperfusion had significantly lower ipsilateral ASL scores compared with those without hyperperfusion ($p < 0.001$, Fig. 4a). According to the results of univariable analysis (Table 1), age, sex, large artery atherosclerosis stroke, and lacunes were entered into multivariate models as covariables. Multivariate regression analysis showed that the ASL score was independently associated with cerebral hyperperfusion after CEA ($p < 0.001$, Table 3). The ASL score was negatively correlated with Log HI ($r = -0.69$, $p < 0.001$, Fig. 4e).

The degree of stenosis, type of CoW, and leptomeningeal collaterals were also associated with cerebral hyperperfusion ($p < 0.001$, Fig. 4b–d). ROC curve analysis revealed that the predictive ability for cerebral hyperperfusion was statistically higher for the ASL score (AUC = 0.98, 95% CI [0.918–0.997]) than for degree of stenosis (AUC = 0.77, 95% CI [0.667–0.854], $p < 0.001$), type of CoW (AUC = 0.784, 95% CI [0.682–0.866], $p = 0.004$), or leptomeningeal collaterals (AUC = 0.78, 95% CI [0.677–0.862], $p = 0.001$). The

AUC for the ASL score was higher than that for the combination of degree of stenosis, type of CoW, and leptomeningeal collaterals (AUC = 0.954, 95% CI [0.886, 0.987]), but this difference did not reach statistical significance ($p = 0.387$). The optimal cutoff value of the ASL score (≤ 25) predicted postoperative cerebral hyperperfusion with 94.1% sensitivity and 88.4% specificity (Fig. 4f). The positive predictive value was 66.7%, and the negative predictive value was 98.4%.

Two representative patients who developed cerebral hyperperfusion/CHS are shown in Figs. 5 and 6.

Patients diagnosed with CHS

Of the 17 patients with post-CEA cerebral hyperperfusion, 3 developed CHS. Two patients developed CHS within 7 days after CEA before discharge, while another patient developed ipsilateral severe throbbing headache, weakness of the left limb, seizure, and coma 24 days after CEA (Fig. 6). After strict control of blood pressure (BP) and lowering of intracranial pressure, hemorrhagic stroke did not occur in these patients. CHS patients had a higher systolic BP at the onset (Table S2-3).

Discussion

In the present study, we demonstrated that the ATA–based ASL score was a comprehensive imaging marker that can reflect the hemodynamic disorders related to the degree of stenosis, and primary and secondary collaterals. This ATA–based ASL score can independently predict cerebral hyperperfusion after CEA.

Table 1 Demographic and imaging characteristics of patients

	All (n=86)	Hyperperfusion	
		No (n = 69)	Yes (n = 17)
Age, years	65.3 ± 7.1	65.5 ± 7.2	64.4 ± 6.6
Male	65 (75.6)	50 (72.5)	15 (88.2)
Risk factors			
Presence of symptoms	32 (37.2)	24 (34.8)	8 (47.1)
TIA	15 (17.4)	13 (18.8)	2 (11.8)
Ischemic stroke	17 (19.8)	11 (15.9)	6 (35.3)
Days escaped since the last ischemic event	0 [0, 30]	0 [0, 27]	5 [0, 45]
Hypertension	63 (73.3)	49 (71)	14 (82.4)
BP_baseline, mmHg	139.7 ± 17.6	138.9 ± 17.2	143.1 ± 19.2
BP_post, mmHg	139.7 ± 12.1	139.5 ± 12	140.5 ± 12.9
Diabetes	35 (40.7)	27 (39.1)	8 (47.1)
Hyperlipidemia	42 (48.8)	32 (46.4)	10 (58.8)
Coronary artery disease	21 (24.4)	15 (21.7)	6 (35.3)
Smoking	42 (48.8)	33 (47.8)	9 (52.9)
Alcohol	20 (23.3)	17 (24.6)	3 (17.6)
Contralateral stenosis ≥ 70%	11 (12.8)	7 (10.1)	4 (23.5)
Large artery atherosclerosis stroke[a], *	18 (20.9)	10 (14.5)	8 (47.1)
Lacunes[a], *	42 (48.8)	29 (42)	13 (76.5)
Shunt use	50 (58.1)	40 (58)	10 (58.8)
Days between CEA and post-surgery MRI	4 [3, 5]	4 [3, 5]	4 [3, 6.5]
Intravenous antihypertensive drugs	21 (24.4)	18 (26.1)	3 (17.6)
Mannitol or glycerol fructose	20 (23.3)	15 (21.7)	5 (29.4)
ASL score and relevant imaging factors			
ASL score*	28 [25, 30]	28 [27, 30]	19 [13, 23]
Degree of stenosis*			
Moderate stenosis	9 (10.5)	9 (13)	0 (0)
Severe stenosis	60 (69.8)	53 (76.8)	7 (41.2)
Near occlusion	17 (19.8)	7 (10.1)	10 (58.8)
Circle of Willis*			
Type 1	15 (17.4)	14 (20.3)	1 (5.9)
Type 2	31 (36)	29 (42)	2 (11.8)
Type 3	7 (8.1)	1 (1.4)	6 (35.3)
Type 4	33 (38.4)	25 (36.2)	8 (47.1)
Opening of leptomeningeal collaterals*	12 (14)	2 (2.9)	10 (58.8)

Normally distributed metric variables were expressed as means ± SD. Non-normally distributed variables were expressed as median [interquartile range]. Categorical variables were expressed as percentages of patients who satisfied the criteria

TIA transient ischemic attack, *BP_baseline* baseline systolic blood pressure measured on admission, *BP_post* maximum systolic blood pressure measured within 7 days after surgery

*Variables with $p < 0.05$ between groups

[a] TOAST classification for ischemic stroke

The advantages of this ATA–based ASL score were that ASL images can be non-invasively obtained using most clinical MRI scanners with the time consumption less than 5 min, and ATA was easy to collect from the original ASL images without complicated post-processing steps. Moreover, carrying out this ATA–based ASL score in patients with carotid stenosis should be reliable. Both the inter-observer and intra-observer agreements for the ASL score performed well in our study. Two other studies using this ASL score in carotid-stenosis patients reached even excellent inter-

**Table 2** Association between ASL score and degree of stenosis and primary and secondary collaterals

	ASL score				*p* value
Leptomeningeal collaterals	Yes (*n* = 12) 19 [14.5, 23]	No (*n* = 74) 28 [26, 30]			< 0.001
Degree of stenosis	Moderate stenosis (*n* = 9) 28 [28, 29.5]	Severe stenosis (*n* = 60) 28 [26, 30]	Near occlusion (*n* = 17) 23 [18, 27]a		0.001
Circle of Willis	Type 1 (*n* = 15) 29 [27, 30]	Type 2 (*n* = 31) 28 [27, 29]	Type 3 (*n* = 7) 19 [16, 23]b	Type 4 (*n* = 33) 27 [24.5, 30]	0.001

ASL scores were expressed as median [interquartile range]

[a] Patients with carotid near occlusion had lower ASL scores than those with moderate stenosis (adjusted *p* = 0.01) and those with severe stenosis (adjusted *p* = 0.003)

[b] Patients with type 3 circle of Willis had significantly lower ASL scores than those with type 1 (adjusted *p* = 0.001), type 2 (adjusted *p* = 0.003), and type 4 (adjusted *p* = 0.028)

Fig. 4 Association between MR imaging features and cerebral hyperperfusion. **a–d** Arterial spin labeling (ASL) score, degree of stenosis, status of primary and secondary collaterals, comparison between patients with and without hyperperfusion. **e** The relationship between ASL score and Log HI (hyperperfusion index). **f** Receiver operating characteristic curves show sensitivity and specificity in the prediction of cerebral hyperperfusion with MR imaging features
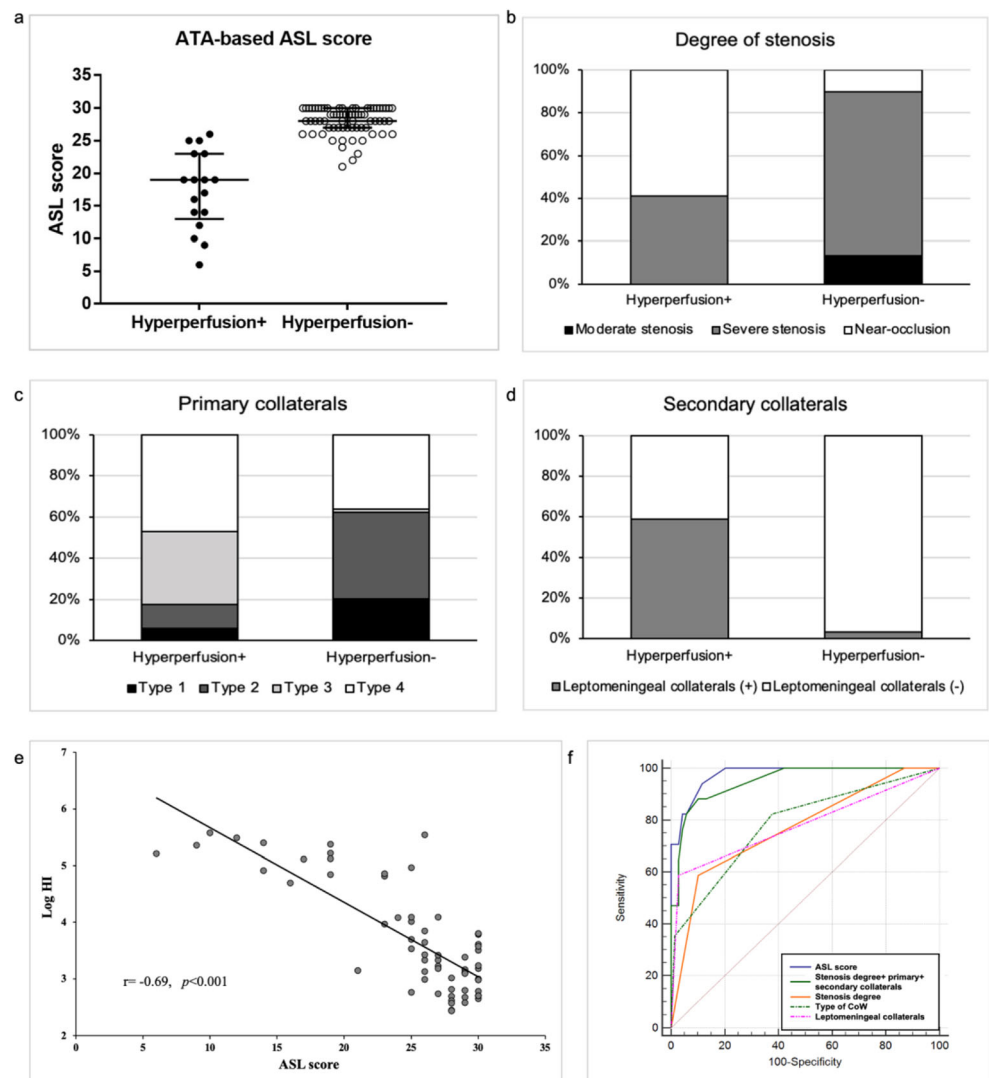
Table 3 Multivariable logistic regression analysis for predictors of postoperative cerebral hyperperfusion

Risk factors	Univariable p value	Multivariable p value	OR (95% CI), B value
ASL score	< 0.001	< 0.001	0.48 (0.33, 0.71), − 0.73
Age	0.579	0.294	NA
Sex, male	0.221	0.899	NA
Large artery atherosclerosis stroke	0.006	0.835	NA
Lacunes	0.011	0.068	NA

OR odds ratio, *CI* confidence interval

observer agreements (κ = 0.76 and 0.91) [30, 31]. Therefore, ASL may be a useful tool that can be applied to routine clinical work for predicting cerebral hyperperfusion after CEA in carotid stenosis.

The optimal value of the ASL score for predicting cerebral hyperperfusion was ≤ 25 in the study, with high sensitivity, specificity, and positive predictive value. The relatively lower negative predictive value may be explained by the low incidence of hyperperfusion. ATAs represent labeled blood that has not reached the microvascular bed at the time of imaging, which occurs when the arterial transit time exceeds PLD [14]. Thus, when referring to this ASL score optimal value, it is necessary to take PLD into account. Also, the conspicuity of ATAs differs at 1.5-T and 3.0-T field strengths because of changes in the blood T1 [32]. We performed this pseudo-continuous ASL protocol with the PLD of 2025 ms on a 3.0-T MRI scanner, which was consistent with the consensus of the ISMRM Perfusion Study Group and the European ASL in Dementia consortium [33]. Therefore, our result may be widely applicable for patients undergoing standard pseudo-continuous ASL.

We found both the degree of stenosis and collaterals were associated with the ASL score, and that may explain why the ASL score can predict hyperperfusion. In terms of degree of stenosis, Di Napoli et al found the presence of ATAs can distinguish moderate and severe stenosis [30]. But they did not report patients with carotid near occlusion, which is often overlooked by radiologists (only 20% sensitivity was reported) and needs to be distinguished from conventional ≥ 50% stenosis [22]. Our study further subdivided the near-occlusion group and showed patients with carotid near occlusion had even lower ASL scores than those with severe stenosis. That indicates the ASL score can distinguish the hemodynamic impairment caused by severe stenosis and near occlusion. More severe stenosis (≥ 87%) and carotid near occlusion are risk factors for hyperperfusion after carotid revascularization [34, 35].

Cerebral collateral flow patterns are commonly divided into primary and secondary collateral pathways. Arterial segments of the CoW are primary collaterals and leptomeningeal vessels are secondary collaterals. Consistent with a previous study [10], we found incomplete anterior semicircle of the CoW was related to lower ASL scores. CoW structures lacking collateral pathways from the contralateral carotid artery were at high risk of postoperative hyperperfusion [19, 20]. Interestingly, in our patients with incomplete anterior semicircles, the presence of ipsilateral PCom was also linked with a lower ASL score. That suggests in the case of incomplete anterior semicircle, the opening of PCom was a marker of impaired cerebral hemodynamics. The previous study [20] found the presence of PCom did not suggest a stable hemodynamic change after surgery. Our results were partly consistent with their study. In addition, we found the presence of secondary leptomeningeal collaterals was also associated with lower ASL scores. The development of leptomeningeal collaterals strongly correlates with reduced CVR in patients with carotid stenosis [16]. That makes sense of the predictive ability of the ASL score for cerebral hyperperfusion.

Based on our finding that the ASL score contained comprehensive hemodynamic information about the degree of stenosis and primary and secondary collaterals, it was not surprising that the ASL score performed better than the degree of stenosis, type of CoW, and leptomeningeal collaterals as well as the combination of the three factors for the prediction of hyperperfusion. That means using ASL alone can predict the occurrence of hyperperfusion; thus, ASL technology enables more cost-effective and streamlined identification of high-risk patients.

In the present study, a new method was adopted to define hyperperfusion by calculating HI. We compared preoperative and postoperative CBF on the voxel-to-voxel level. Due to the relatively low signal-to-noise ratio of ASL images [33], we only included clusters more than 100 mm3 as effective hyperperfusion regions. Moreover, the watershed area is especially susceptible to ischemia and hypoperfusion; thus, patients in the non-hyperperfusion group may still have some "hyperperfusion voxels" (e.g., Fig. 2a, case 1). Crucially, hyperperfusion regions in the watershed area are small, whereas hyperperfusion after CEA due to impaired CVR has a territory effect [36]. Based on the concept of territory effect, patients with hyperperfusion should have a more extensive and serious increase in perfusion than those without hyperperfusion [1, 3].
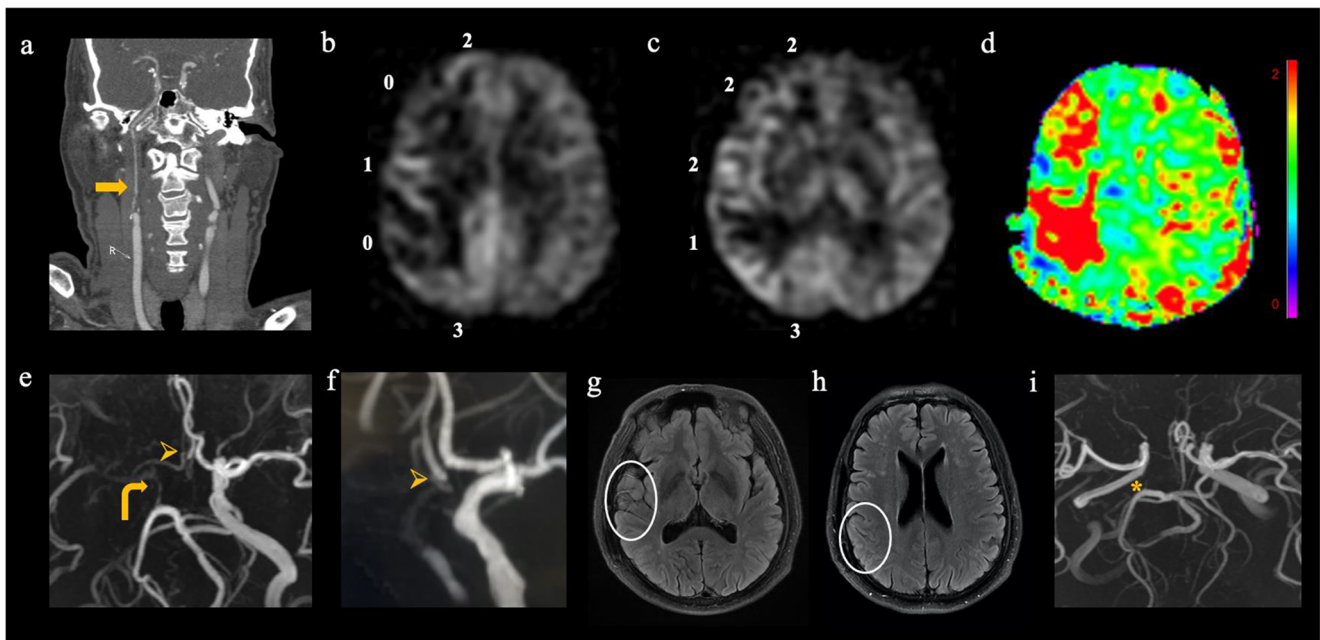
Fig. 5 A representative case of cerebral hyperperfusion symptom (CHS). a A patient with right carotid stenosis. b, c Arterial spin labeling (ASL) score based on arterial transit artifacts on two slices corresponding to the ASPECT score locations. The total ASL score was 16 points. d Cerebral blood flow ratio map shows hyperperfusion in the ipsilateral middle cerebral artery territory. Preoperative computed tomography angiography (a), MR angiography (e, f), and fluid-attenuated inversion recovery (g, h) show carotid near occlusion (arrow), absence of the anterior communicating artery (arrowhead), opening of the ipsilateral posterior communicating artery (curved arrow), and leptomeningeal collaterals (oval). i Postoperative MR angiography shows a decrease in the signal of the ipsilateral posterior communicating artery (asterisk) after surgery. This patient further developed CHS
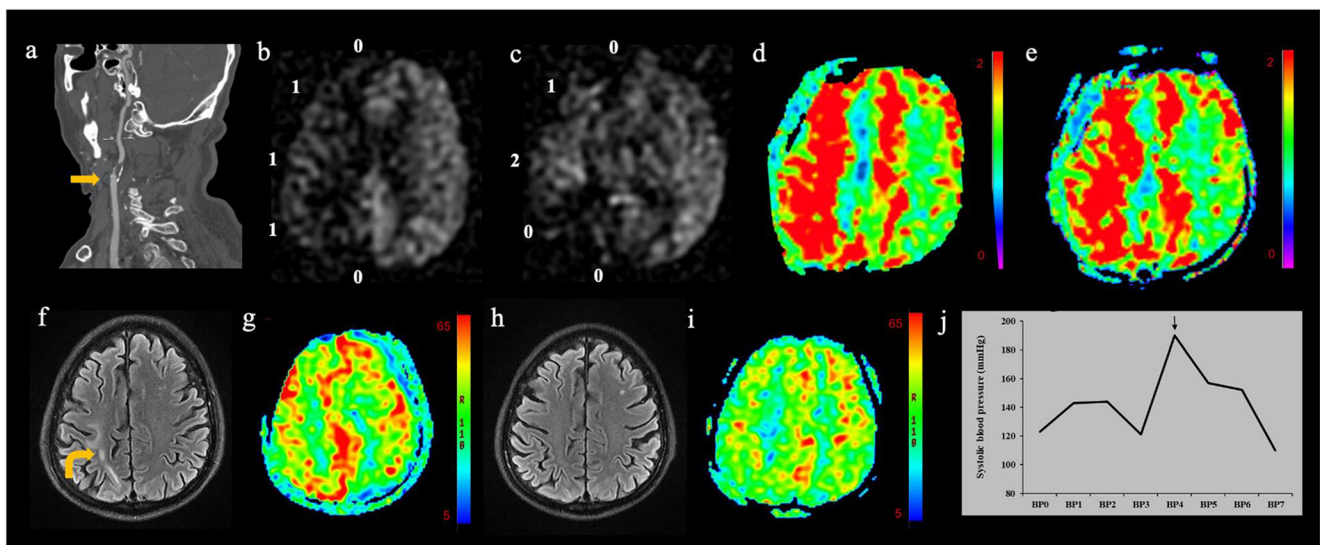
Fig. 6 A case of late-onset cerebral hyperperfusion symptom (CHS). a Computed tomography angiography shows right carotid artery severe stenosis (arrow). The preoperative arterial spin labeling (ASL) score was 6 points (b, c), and cerebral hyperperfusion was determined by cerebral blood flow (CBF) ratio maps (d, e). This patient had no symptoms or signs related to CHS during the first hospitalization. On the 24th day after surgery, the patient was re-admitted to hospital due to CHS with a systolic blood pressure of 190 mmHg. Fluid attenuation inversion recovery (f) shows regional swelling of the ipsilateral parietal and occipital lobe (curved arrow), and the CBF of the right occipital lobe was higher than that of the left (g). After treatment, the regional swelling disappeared (h) and the CBF of the right occipital lobe decreased to normal (i). j Changes in systolic blood pressure during two hospitalizations. BP0, baseline blood pressure; BP1, blood pressure within 24 h after surgery; BP2, maximum blood pressure after surgery during the first hospitalization; BP3, blood pressure at the first discharge; BP4, blood pressure on re-admission (down arrow); BP5, blood pressure within 24 h of re-admission; BP6, maximum blood pressure after 24 h during the second hospitalization; BP7, blood pressure at the second discharge

The phenomenon of significantly higher HIs in the last 17 patients demonstrated that our method can effectively distinguish patients with and without hyperperfusion.

According to previous studies, the incidence of cerebral hyperperfusion was 9–14% [37]. The incidence of CHS ranged from 0.2 to 18.9%, and most studies reported incidences between 0 and 3% [2]. Compared with previous studies, the incidence of cerebral hyperperfusion (19.8%) and CHS (3.5%) were higher in the present study. One reason may be that patients with carotid near occlusion, for whom the treatment strategy is still controversial [38], received CEA in our hospital. This group of vulnerable patients was usually treated by medical treatment [38] and not often included or mentioned for analysis in previous hyperperfusion studies [1, 3, 4, 7]. Moreover, CBF was often measured by placing a region of interest in the whole middle cerebral artery territory from a single axial image slice in previous studies [1, 3, 8, 10], which cannot provide a full view of hyperperfusion regions stereoscopically. Hyperperfusion regions perpendicular or angulated to the axis may fail to be detected. The present study quantified the hyperperfusion volume by automation in the voxel level, providing a more accurate and sensitive method for detecting hyperperfusion in the entire brain without any operator bias.

Our study had some limitations. First, DSA was the reference standard method for evaluating leptomeningeal collaterals but it was not performed in our patients due to the invasiveness. In order to detect leptomeningeal collaterals more sensitively on FLAIR images, long repetition and echo times (TR = 12,000 ms, TE = 122 ms) were adopted for an excellent contrast between the cerebrospinal fluid and brain surface [39]. Second, a technical limitation is the labeling duration of 1450 ms, which is slightly shorter than the 1800 ms recommended by the white paper [32]. The shorter labeling duration did not affect the conspicuity of ATAs, but may lead to a reduced ASL signal. Therefore, the possibility that we got a lower ASL score cannot be ruled out. Third, although we adopted relatively standard ASL parameters, ASL is implemented in different ways among different vendors. Future studies that perform standard ASL on other vendors are needed to confirm our results. Fourth, the definition of hyperperfusion varied from one method to another. This preliminary ASL method for the detection of cerebral hyperperfusion needs to be verified by future studies. Fifth, the prediction of CHS may be more clinically valuable than that of cerebral hyperperfusion. The sample size was relatively small for the analysis of CHS because of its low incidence.

In conclusion, ATA on ASL MRI is a practical imaging marker that can be obtained by visual inspection without complex post-processing steps. Based on the presence of ATA, preoperative ASL can predict cerebral hyperperfusion after CEA in patients with carotid stenosis. Our findings support the application of ASL technology in clinical practice for the risk assessment of postoperative complications in carotid stenosis.

Declarations

Guarantor The scientific guarantor of this publication is Feng Feng.

Conflict of interest The authors of this manuscript declare that they have no conflict of interest.

Statistics and biometry No complex statistical methods were necessary for this paper.

Informed consent Written informed consent was obtained from all patients in this study.

Ethical approval This prospective study was approved by the Medical Ethics Committee of the Peking Union Medical College Hospital.

Study subjects or cohorts overlap Some study subjects or cohorts have been previously reported in:
• Lin T, Lai Z, Lv Y, et al (2018) Effective collateral circulation may indicate improved perfusion territory restoration after carotid endarterectomy. Eur Radiol 28:727–735.
• Lin T, Lai Z, Zuo Z et al (2019) ASL perfusion features and type of circle of Willis as imaging markers for cerebral hyperperfusion after carotid revascularization: a preliminary study. Eur Radiol 29:2651-2658.
• Fan X, Zhang X, Lai Z et al (2021) Cerebral small vessel disease burden related to carotid intraplaque hemorrhage serves as an imaging marker for clinical symptoms in carotid stenosis. Front Neurol 12:731237.
• Fan X, Lai Z, Lin T et al (2021) Pre-operative cerebral small vessel disease on MR imaging is associated with cerebral hyperperfusion after carotid endarterectomy. Front Cardiovasc Med 8:734392.

Methodology
• prospective
• observational
• performed at one institution

References

1. Ogasawara K, Yukawa H, Kobayashi M et al (2003) Prediction and monitoring of cerebral hyperperfusion after carotid endarterectomy using single-photon emission computerized tomography scanning. J Neurosurg 99:504–510
2. van Mook WN, Rennenberg RJ, Schurink GW et al (2005) Cerebral hyperperfusion syndrome. Lancet Neurol 4:877–888
3. Komoribayashi N, Ogasawara K, Kobayashi M et al (2006) Cerebral hyperperfusion after carotid endarterectomy is associated

with preoperative hemodynamic impairment and intraoperative ce-rebral ischemia. J Cereb Blood Flow Metab 26:878–884

4. Hosoda K, Kawaguchi T, Shibata Y et al (2001) Cerebral vasoreactivity and internal carotid artery flow help to identify pa-tients at risk for hyperperfusion after carotid endarterectomy. Stroke 32:1567–1573

5. Spano VR, Mandell DM, Poublanc J et al (2013) CO2 blood oxy-gen level-dependent MR mapping of cerebrovascular reserve in a clinical population: safety, tolerability, and technical feasibility. Radiology 266:592–598

6. Saito H, Ogasawara K, Suzuki T, Kuroda H, Kobayashi M, Yoshida K et al (2011) Adverse effects of intravenous acetazol-amide administration for evaluation of cerebrovascular reactivity using brain perfusion single-photon emission computed tomogra-phy in patients with major cerebral artery steno-occlusive diseases. Neurol Med Chir 51:479–483

7. Fassaert LMM, Immink RV, van Vriesland DJ et al (2019) Transcranial Doppler 24 hours after carotid endarterectomy accu-rately identifies patients not at risk of cerebral hyperperfusion syn-drome. Eur J Vasc Endovasc Surg 58:320–327

8. Yamauchi K, Enomoto Y, Otani K, Egashira Y, Iwama T (2018) Prediction of hyperperfusion phenomenon after carotid artery stenting and carotid angioplasty using quantitative DSA with cere-bral circulation time imaging. J Neurointerv Surg 10:576–579

9. Iwata T, Mori T, Tanno Y, Kasakura S, Yoshioka K (2018) Measurement of oxygen extraction fraction by blood sampling to estimate severe cerebral hemodynamic failure and anticipate cere-bral hyperperfusion syndrome following carotid artery stenting. J Neurointerv Surg 10:1063–1066

10. Nakagawa I, Yokoyama S, Wajima D et al (2019) Hyperventilation and breath-holding test with indocyanine green kinetics predicts cerebral hyperperfusion after carotid artery stenting. J Cereb Blood Flow Metab 39:901–912

11. Donahue MJ, Strother MK, Hendrikse J (2012) Novel MRI ap-proaches for assessing cerebral hemodynamics in ischemic cerebro-vascular disease. Stroke 43:903–915

12. Uchihashi Y, Hosoda K, Zimine I et al (2011) Clinical application of arterial spin-labeling MR imaging in patients with carotid steno-sis: quantitative comparative study with single-photon emission CT. AJNR Am J Neuroradiol 32:1545–1551

13. Zaharchuk G, Do HM, Marks MP, Rosenberg J, Moseley ME, Steinberg GK (2011) Arterial spin-labeling MRI can identify the presence and intensity of collateral perfusion in patients with moyamoya disease. Stroke 42:2485–2491

14. Bang OY, Goyal M, Liebeskind DS (2015) Collateral circulation in ischemic stroke: assessment tools and therapeutic strategies. Stroke 46:3302–3309

15. Lee S, Yun TJ, Yoo RE et al (2018) Monitoring cerebral perfusion changes after revascularization in patients with Moyamoya disease by using arterial spin-labeling MR Imaging. Radiology 288:565–572

16. Kunieda T, Miyake K, Sakamoto H et al (2017) Leptomeningeal collaterals strongly correlate with reduced cerebrovascular reactiv-ity measured by acetazolamide-challenged single-photon emission computed tomography using a stereotactic extraction estimation analysis in patients with unilateral internal carotid artery stenosis. Intern Med 56:2857–2863

17. de Boorder MJ, van der Grond J, van Dongen AJ et al (2006) Spect measurements of regional cerebral perfusion and carbondioxide reactivity: correlation with cerebral collaterals in internal carotid artery occlusive disease. J Neurol 253:1285–1291

18. Roach BA, Donahue MJ, Davis LT et al (2016) Interrogating the functional correlates of collateralization in patients with intracranial stenosis using multimodal hemodynamic imaging. AJNR Am J Neuroradiol 37:1132–1138

19. Liang F, Fukasaku K, Liu H, Takagi S (2011) A computational model study of the influence of the anatomy of the circle of Willis on cerebral hyperperfusion following carotid artery surgery. Biomed Eng Online 10:84

20. Katano H, Mase M, Sakurai K, Miyachi S, Yamada K (2012) Revaluation of collateral pathways as escape routes from hyperemia/hyperperfusion following surgical treatment for carotid stenosis. Acta Neurochir 154:2139–2148 discussion 2148-2149

21. North American Symptomatic Carotid Endarterectomy Trial Collaborators, HJM B, Taylor DW et al (1991) Beneficial effect of carotid endarterectomy in symptomatic patients with high-grade carotid stenosis. N Engl J Med 325:445–453

22. Johansson E, Gu T, Aviv RI, Fox AJ (2020) Carotid near-occlusion is often overlooked when CT angiography is assessed in routine practice. Eur Radiol 30:2543–2551

23. Bartlett ES, Walters TD, Symons SP, Fox AJ (2006) Diagnosing carotid stenosis near-occlusion by using CT angiography. AJNR Am J Neuroradiol 27:632–637

24. Maas MB, Lev MH, Ay H et al (2009) Collateral vessels on CT angiography predict outcome in acute ischemic stroke. Stroke 40:3001–3005

25. Horie N, Morikawa M, Morofuji Y et al (2014) De novo ivy sign indicates postoperative hyperperfusion in moyamoya disease. Stroke 45:1488–1491

26. Mori N, Mugikura S, Higano S et al (2009) The leptomeningeal "ivy sign" on fluid-attenuated inversion recovery MR imaging in Moyamoya disease: a sign of decreased cerebral vascular reserve? AJNR Am J Neuroradiol 30:930–935

27. Liu W, Xu G, Yue X et al (2011) Hyperintense vessels on FLAIR: a useful non-invasive method for assessing intracerebral collaterals. Eur J Radiol 80:786–791

28. Fahlstrom M, Lewen A, Enblad P, Larsson EM, Wikstrom J (2020) High intravascular signal arterial transit time artifacts have negligi-ble effects on cerebral blood flow and cerebrovascular reserve ca-pacity measurement using single postlabel delay arterial spin-labeling in patients with moyamoya disease. AJNR Am J Neuroradiol 41:430–436

29. Lin T, Qu J, Zuo Z, Fan X, You H, Feng F (2020) Test-retest reliability and reproducibility of long-label pseudo-continuous ar-terial spin labeling. Magn Reson Imaging 73:111–117

30. Di Napoli A, Cheng SF, Gregson J et al (2020) Arterial spin label-ing MRI in carotid stenosis: arterial transit artifacts may predict symptoms. Radiology 297:652–660

31. Lin TY, Lai ZC, Lv YL et al (2018) Effective collateral circulation may indicate improved perfusion territory restoration after carotid endarterectomy. Eur Radiol 28:727–735

32. Zaharchuk G (2020) Arterial transit awesomeness. Radiology 297:661–662

33. Alsop DC, Detre JA, Golay X et al (2015) Recommended imple-mentation of arterial spin-labeled perfusion MRI for clinical appli-cations: a consensus of the ISMRM perfusion study group and the European consortium for ASL in dementia. Magn Reson Med 73:102–116

34. Cay F, Cil BE, Balci S, Arsava EM, Topcuoglu MA, Arat A (2020) Relevance of distal arterial collapse in stenting of atherosclerotic near-occlusion of the carotid artery. AJNR Am J Neuroradiol 41:1054–1060

35. Ohta T, Nakahara I, Matsumoto S et al (2017) Prediction of cerebral hyperperfusion after carotid artery stenting by cerebral angiography and single-photon emission computed tomography without acet-azolamide challenge. Neurosurgery 81:512–519

36. Markus H, Cullinane M (2001) Severely impaired cerebrovascular reactivity predicts stroke and TIA risk in patients with carotid artery stenosis and occlusion. Brain 124:457–467

37. Adhiyaman V, Alexander S (2007) Cerebral hyperperfusion syn-drome following carotid endarterectomy. QJM 100:239–244

38. de Borst GJ, Antonopoulos CN, Meershoek AJA, Liapis CD (2020) Carotid artery near occlusion: time to rethink the management? Eur J Vasc Endovasc Surg 60:169–170

39. Iancu-Gontard D, Oppenheim C, Touzé E et al (2003) Evaluation of hyperintense vessels on FLAIR MRI for the diagnosis of multiple intracerebral arterial stenoses. Stroke 34:1886–1891

Publisher's note Springer Nature remains neutral with regard to jurisdictional claims in published maps and institutional affiliations.